

Research Paper

# The effect of water boundary conditions of advance face and lining on the evolution of internal forces in lining

J. Song<sup>1</sup>, L. Miao<sup>2</sup> and S. Feng<sup>3</sup>

## ARTICLE INFORMATION

### Article history:

Received: 15 November, 2014

Received in revised form: 27 April, 2015

Accepted: 05, May, 2015

Published on: June, 2015

### Keywords:

Water boundary condition

Internal forces in lining

Coupled mechanical and hydraulic analysis

Pore water pressure

Tunnel excavation

## ABSTRACT

After tunnel excavation and lining installed, the excess pore pressures around tunnel dissipate over time, thus changing the soil effective stresses and leading to additional, time-dependent deformations. The deformation of soil around the tunnel can change the internal forces in lining. This study focuses on the effect of boundary conditions of advance face and lining on the internal forces in lining after tunnel excavation. The numerical model with specific geological conditions is established and the tunneling process is modeled by a step-by-step excavation using ABAQUS software. Four different cases were considered in the numerical model including permeable or impermeable boundary conditions of the lining and the advance face. From the calculation result the change mechanism of the internal forces in the lining after tunnel excavation are obtained. When the lining is impermeable the internal forces in the lining changes a little after tunnel excavation and when the lining is permeable the internal forces increased is dramatic. When the advance face is impermeable the increased internal forces in the lining are larger and when the tunnel is buried in large permeably soil the internal forces in the lining will be constant after tunnel excavation.

## 1. Introduction

Tunnel excavation generates excess pore pressures around the lining. The excess pore pressures dissipate over the course of time, thereby changing the effective stresses and leading to additional time-dependent deformations. Field measurements show clearly that settlements induced by tunnelling through low-permeability clay deposits may increase for several months after excavation. As a result, the load acting on the lining will change over time while the lining hinders ground deformations.

The lining of sealed tunnels is designed to withstand hydrostatic pressures and the earth pressures. For the

design of the lining underwater, estimations of the force acting on the lining and the stress in the lining after tunnel excavation due to consolidation of soil must be considered. Usually two approaches, numerical methods and analytical methods, are used to estimate the soil pressure and the lining stresses in an underwater tunnel. Many researches have been done on this problem. For deep tunnels, Atkinson and Mair (1983) mentioned that, using an elastic approach, loads on the tunnel linings are the same, considering impermeable or fully-drained lining. For shallow tunnels, Schweiger (1991) and Lee (2001) obtained less stresses in the linings with the consideration of the seepage force. Ponlawich (2009) investigated the effect of drainage conditions on pore-

<sup>1</sup> School of civil engineering, Henan University of Urban Construction, Pingdingshan 467044, CHINA, cumtsong@163.com

<sup>2</sup> Institute of Geotechnical Engineering, southeast University, Nanjing 210096, CHINA, Lc.miao@seu.edu.cn

<sup>3</sup> School of civil engineering, Henan University of Urban Construction, Pingdingshan 467044, CHINA, shengshengdu@163.com

Note: Discussion on this paper is open until September 2015

water pressure distributions and lining stresses in drained tunnels. Schmitt (2009) investigated the behaviour of single shielded TBMs by means of fully three-dimensional, step-by-step simulations of tunnel excavation, thus gaining a valuable insight into the effects of non-uniform convergence and of non hydrostatic shield and lining loading.

After the excavation of the shield, the pore water pressure around the tunnel is formulate. The distribution form of the pore water pressure is not always the same. (Anagnostou and Kovári , 1996; Anagnostou, 2005).The water boundary conditions of advance face and lining can affect the distribution form of pore water pressure around the tunnel. Thus the internal forces in lining will be affected by it too.

The continuous increase of efficiency of modern computer technology and the considerable progress in computational structural mechanics have stimulated the development of numerical simulation models in tunneling. Compared to the large number of models developed in the context of NATM tunneling only a relatively small number of mature numerical models is existing for shield tunneling due to its more complex nature. First 3D finite element models for shield tunneling have been developed by Lee and Rowe (2005), assuming undrained soil conditions and using a Mohr–Coulomb material model for the soil. They were improved later by other researchers(Mansour, 1996; Swoboda and Abu-Krishna, 1999; Kasper and Meschke, 2006; Galli, Grimaldi and Leonardi, 2004; Shin and Potts, 2005). A relatively comprehensive 3D finite element model of shield tunnelling has been developed by Mroueh (2008) for drained conditions, using the Mohr–Coulomb model for the soil.

The present paper investigates the distribution form of the pore water pressure around the lining after the excavation of the shield at first. Then the change processes of the internal forces in the lining are investigated. The research work is done with the ABAQUS software by means of hydraulic-mechanical coupled numerical analyses, which account for the highly complex transient process of consolidation around the advancing tunnel face. Results from the calculation are used to evaluate the effects of different water boundary conditions of advance face and lining on the pore water pressure in the soil and the internal forces in the lining.

## 2. Computational model

### 2.1 The model of shield tunneling

The model established in this paper is illustrated in Fig.1 the model includes the soil, the shield machine, the

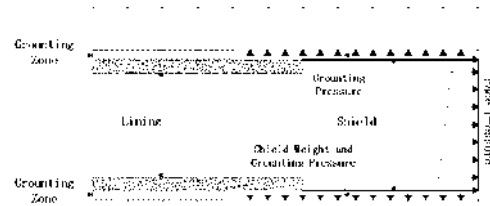


Fig. 1. The calculation model of shield tunneling.

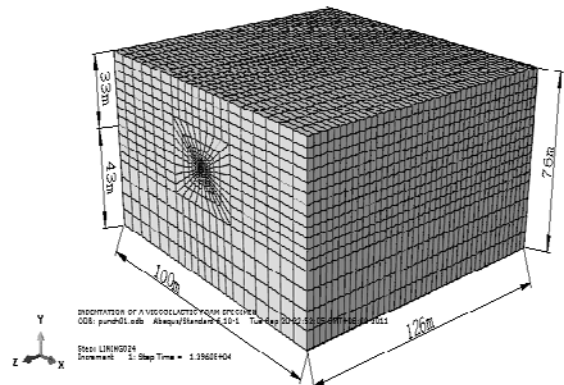


Fig. 2. FE mesh of the numerical model.

Table 1. Material properties used in the numerical analysis.

	$\gamma$ (kN/m <sup>3</sup> )	Void ratio	E (Mpa)	C (kPa)	$\phi'$ (°)	K (m/s)
Ground	19.6	0.9	50	25	20	1e-8
Lining	25	-	35000	-	-	-
Grouting zone	20	0.5	650	-	-	1e-8

face pressure, the grouting pressure, the lining and the grouting zone. The material property of grouting zone is illustrated in Table 1. The face pressure at the tunnel center is 0.2 MPa and the grouting pressure is 0.15 MPa.

### 2.2 Model geometry and boundary conditions

The numerical calculation is made using the finite element software ABAQUS/Standard, which can address the coupled mechanical and hydraulic problems (ABAQUS Consulting Group, 2008). The problem is investigated by means of numerical calculations for a shallow tunnel crossing homogeneous ground.

A model boundary of a sufficient size is very important in a seepage analysis to avoid adverse influence on the analysis results. The model boundaries are located at the flowing ranges to avoid a boundary effect. The dimensions here are as follows: (1) the horizontal range of the model is 10 times the radius of the tunnel; (2) the longitudinal range is approximately 50 times the tunnel radius; (3) the bottom range is approximately 18 times the tunnel radius. The boundary ranges are shown in Fig. 2.

In order to simulate the consolidation phenomenon, elements with eight nodal degrees of freedom were used below the water table, providing quadratic interpolation of displacements and linear interpolation of pore pressures and thereby allowing the calculation of the displacements in eight nodes and the excess pore pressure. So the consolidation processes have been regarded in this analysis. The gradual increase of ground pressure and of ground deformations is therefore considered to be not only due to the spatial stress redistribution that is associated with the progressive advance of the working face, but also to the dissipation of the pore water pressure.

For the boundary condition on the advance face, in the research work of G. Anagnostou (1996), a constant piezometric head  $h_F < h_0$  is prescribed. In the research work of Seung Han Kim on the slurry shield tunnel, the impervious membrane develops when the small clay particles in the slurry form a filter cake on the excavation surface quickly enough to prevent slurry infiltration as soon as the soil mass is removed from the excavation face. In this paper, the piezometric head of the advance face is set to different conditions as illustrated in Fig. 3. In the extreme case, the pressure is atmospheric or the piezometric head equal to the elevation at each point ( $h_2$ ).

For the boundary conditions of the lining, Schweiger (1991) showed that the lining stresses in the drained condition were about 75 % of the value obtained when the full hydrostatic pressure is applied. In drained tunnels, two different boundary conditions (one for zero water pressure and the other for a constant total head) along the tunnel circumference are used in the existing solutions and analyses (Park et al., 2008). Through the comparison of the analytical results for steady-state groundwater inflow and seepage force, Park showed the difference in the predictions of groundwater inflow and seepage force for two different boundary conditions in a shallow drained circular tunnel. Therefore, it is required to investigate the effect of different drainage conditions (sealed, fully-drained, and invert only-drained) on lining stresses.

In this study, two types of tunnels were considered – a drainage type tunnel and a water-proof type tunnel. In case of the drainage type tunnel, it is assumed that groundwater flows into all of the excavated surfaces including the tunnel face. The tunnel construction by NATM can be included in this category. In case of the water-proof type tunnel, the groundwater flows only into the tunnel face. The tunnel construction by the shield can be included in this category.

The boundary conditions of the lining and the advance face used in this research are illustrated in Fig. 3. There are four different cases totally including

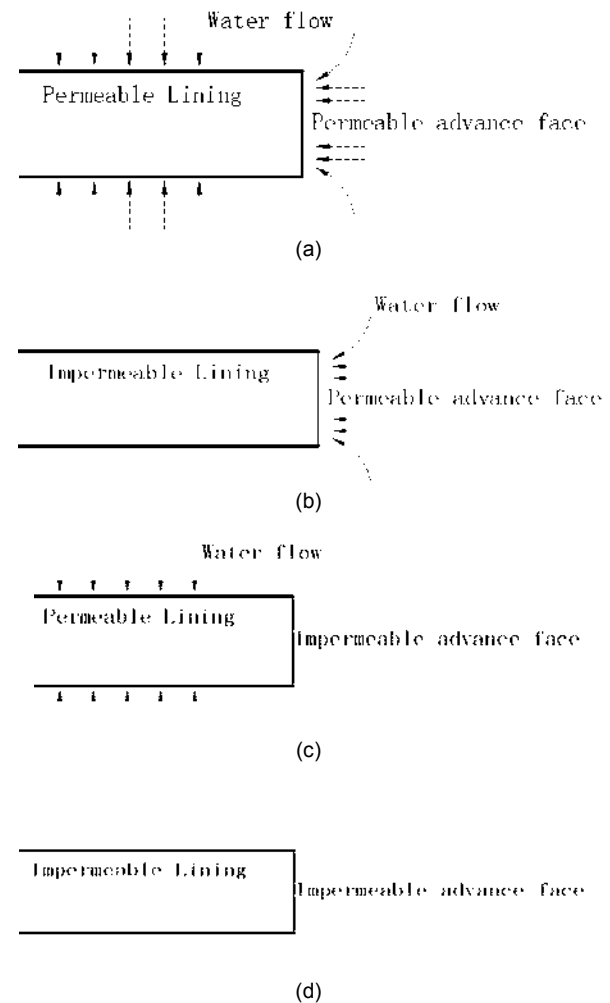


**Fig. 3.** The different water boundary conditions of the lining and advance face.

permeable or impermeable boundary conditions of the lining and the advance face. So the effects of different drainage conditions on pore-water pressure distributions, flow nets, and lining stresses can be investigated.

The total head at the top of the seawater is fixed throughout the analysis due to the infinite inflow of seawater. For the condition of a impermeable lining on the ground surface, the flow into the tunnel was not permitted. For the permeable lining, the pore water at the lining are fixed zero values. The lateral boundary nodes of the finite element mesh are defined as fixed in the horizontal direction and moveable in the vertical direction. The nodes of the lower edge of the model are defined as fixed in both directions. Typical modeling mesh is shown in Fig. 2.

### 2.3 Material properties

Table 1 shows the properties of soil, concrete lining and grouting zone used in the analysis. The ground was assumed to be an elastic perfectly-plastic material

conforming Mohr-Coulomb failure criterion. Solid elements were applied for the simulation of the tunnel lining and grouting zone.

2.4 Analysis procedure

After excavating the tunnel is lined immediately with segment. Each excavation cycle takes a half day and thus the rate of advance amounts 6 m/day. The consolidation is determined by the duration of the excavation cycles, the deformation-induced pore pressure distribution and the hydrostatic pore pressure Biot's theory of coupled consolidation is assumed. The advance of the excavation face is affected by the deactivation of the volume elements within the tunnel cross section. At the same time the pore pressure in the deactivated elements are set to zero.

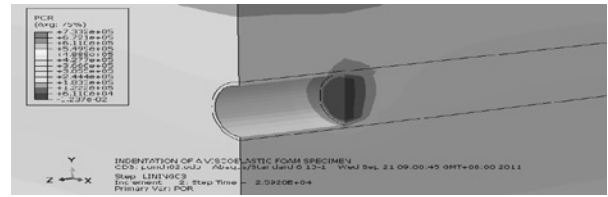
According to the procedure described above 100 excavation cycles with a total length of 100R are modeled. The calculated deformations are considered to be small so that the formulation is referred to the original undeform geometry without performing an updated mesh analysis.

3. Analysis results and discussions

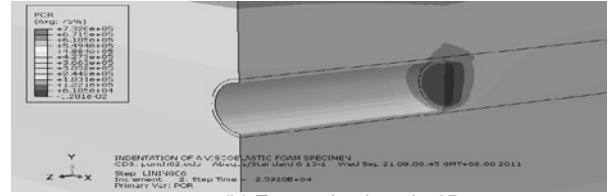
3.1 The result of permeable advance face with impermeable lining

Figure 4 shows the distribution of pore water pressures in the process of tunneling excavation with the boundary conditions of permeably advance face and impermeably lining. It illustrate that the pore water pressure in the soil are influenced by the permeably advance face. The pore water pressure along the axis of tunnel is illustrated in Fig. 5. It can be concluded that the hydraulic head in the vicinity of the tunnel face are nearly the same after three excavations. For example, the pore water pressures in the vicinity of the tunnel face are nearly the same when the excavation length is 9 m and 12 m. This result has a good agreement with Lee (2004). The loss of hydraulic head in the vicinity of the tunnel face does not take place immediately after excavation. In other words, it takes time after tunnel excavation to reach a steady-state hydraulic head distribution.

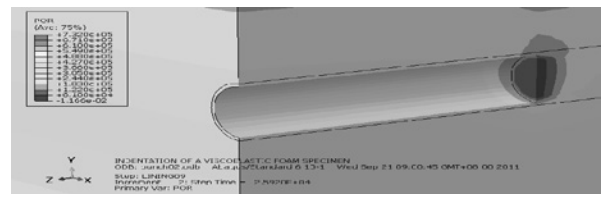
Figure 6 shows the distribution of pore water pressure in the process of tunneling excavation with the boundary conditions of permeably advance face and impermeably lining. The pore water pressure around the tunnel is influenced by the advance face while it recovers soon after the advance face having passed through the monitor section.



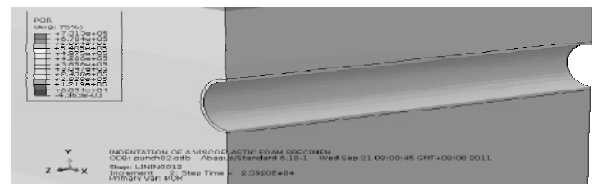
(a) Excavation length=2D.



(b) Excavation length=6D.



(a) Excavation length=10D.



(b) After excavation.

Fig. 4. The pore water pressure distribution at different excavation step with permeable advance face and impermeable lining.

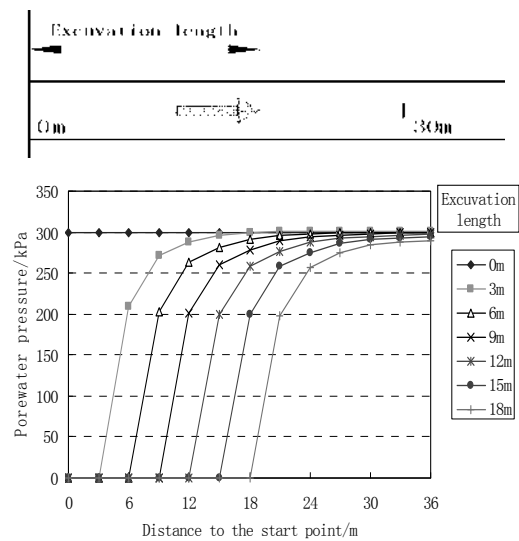


Fig. 5. The pore water pressure along the axis of tunnel.

The evolution of the pore water pressure at different point around the tunnel after excavation is illustrated in Fig. 7. The values increases with time and values at the end of consolidation (T = 15 year) are equal to the initial values without the disturbance of tunnel excavation.

The maximum and minimum moment in the lining at different time are illustrated in Fig. 8. The maximum value of bending moments occurs at the crown and the spring line. The value of maximum and minimum moment decrease a little with time and the difference is smaller than 7 kN·m.

From the result of the model with permeably advance face and impermeably lining, it can be conclude that the pore water pressure around the tunnel are decreased by the advance face after the advance face passing by. Then the pore water pressure recovered with time and as a result the internal forces in the lining decrease with time, but the decreasing value is small. At the end of the soil consolidation, the pore water pressure around tunnel recover to the initial values and the internal forces in the lining keep stable values.

3.2 The result of permeable advance face with permeable lining

Figure 9 shows the distribution of pore water pressures in the process of tunneling excavation with the boundary conditions of permeably advance face and permeably lining. The water pressure around the tunnel is not only influenced by the permeably advance but also by the permeably lining.

The maximum moment in the lining at different time are illustrated in Fig. 10. The moment increased with time significantly. The maximum increased value is lager than 50 kN·m. The pore water pressure along the line on the right of the tunnel at different time is illustrated in Fig. 11. The pore water pressure around the tunnel decreases with time after the tunnel advance face is passing by. The result show good agreement to Ramoni and Anagnostou (2011). To make an insight to the differential settlement between the lining and the soil, the local coordinate system on the top of the tunnel is used as illustrated in Fig. 12. It can be found that there are significant differential settlement between the lining and the soil and the differential settlement increase with time. So it can be conclude that after the tunnel excavation the pore water pressure around the tunnel decrease with time due to the permeable lining. At the same time the differential settlement between the lining and the soil increased due to the decrease of the pore water pressure. So that the internal forces in the lining increased with time.

The permeability of soil can influence the change regulations of the internal forces in the lining. When the

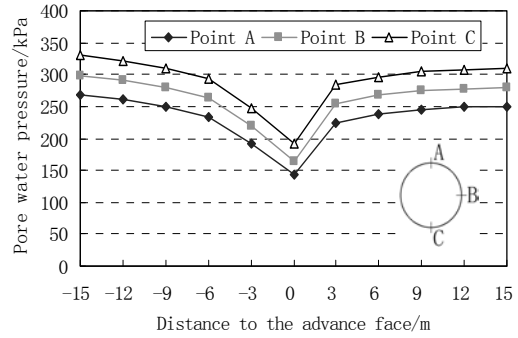


Fig. 6. The evolution of the pore water pressure at different points around the tunnel (When the advance face has not passed through the monitor section the points, the value of distance is negative.).

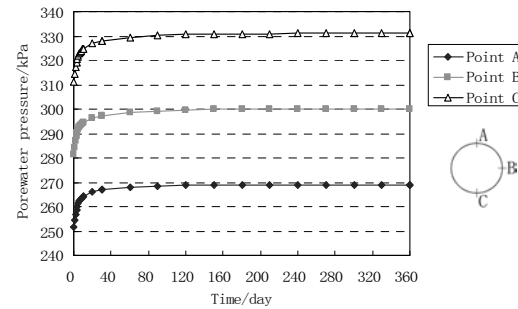
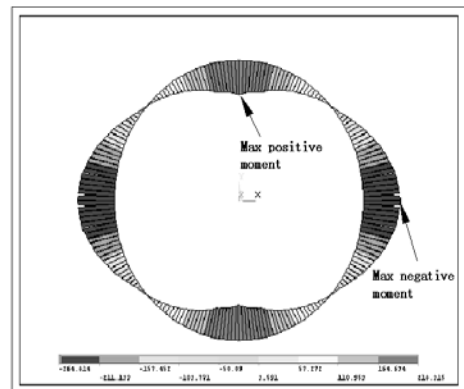
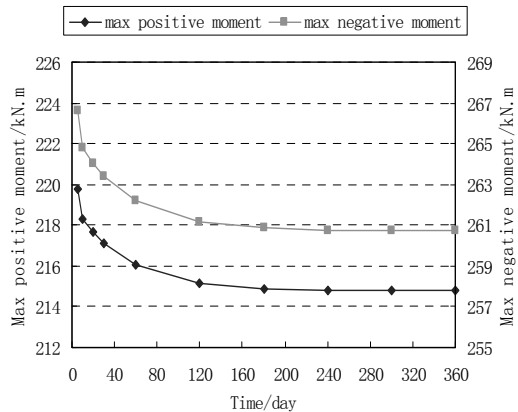


Fig. 7. Pore-water pressure around the lining (with permeable advance face and impermeable lining. T = 0 refer to the end of the tunnel excavation).



(a) Moment in the lining



(b) The maximum and minimum moment in the lining at different time.

permeability of soil is  $1 \times 10^{-6}$  m/s, the calculation result is illustrated in Figs.13 and 14. Because the permeability of soil is large, the consolidation process of the soil is fast. The pore water pressure around the tunnel decreased to the final status quickly after the excavation of the tunnel as illustrated in Fig. 13. And the internal forces in the Lining do not increase with time as illustrated in Fig. 14.

3.3 The result of impermeable advance face with impermeable lining

The pore water pressure around the lining with impermeable advance face and impermeable lining is illustrated in Fig. 15. It can be seen that the pore water pressure around the tunnel is disturbed by the spatial stress redistribution caused by the tunnel excavation. The pore water pressure decreased with time but the decreased value is smaller than 15 kPa (Fig. 16). The internal force increased with time and the increased value is smaller than 2 kN•m (Fig. 17). So when the advance face and the lining are all impermeable, the influence of the tunnel excavation on the internal forces in the lining can be reduced to the minimum.

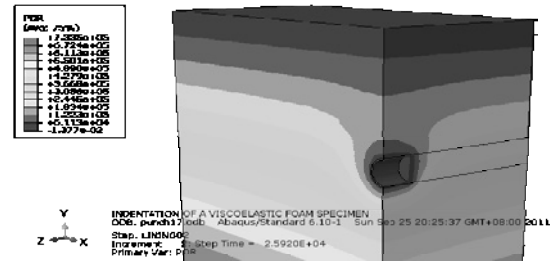
3.4 The result of impermeable advance face with permeable lining

The pore water pressure around the lining with impermeable advance face and impermeable lining is illustrated in Fig. 18. The water pressure around the tunnel is influenced by the permeably lining. The influence result on the pore water pressure in the vicinity of the advance face is less than the result of the model with permeable advance face and permeable lining.

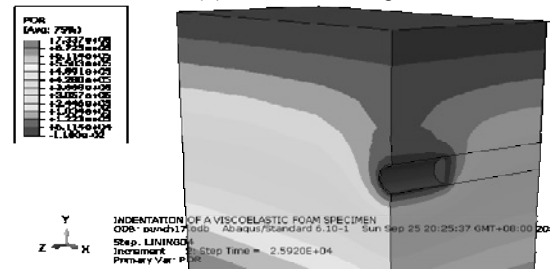
The maximum and minimum moment in the lining at different time are illustrated in Fig. 19. The moment increased with time significantly and the maximum increased value is larger than 70 kN•m. The increased value is larger than the result of the model with permeable advance face and permeable lining. So the permeability of lining should be controlled to avoid water leakage.

3.5 Discussion of the calculation results

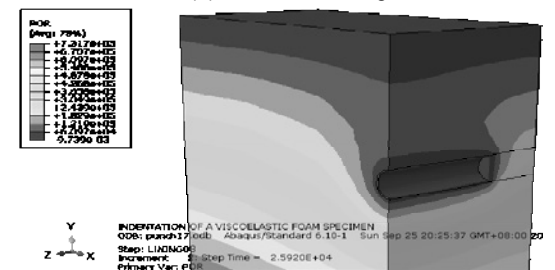
From the calculation result the change mechanism of the internal forces in the lining after tunnel excavation can be obtained. The changes of the internal forces in the lining are due to the consolidation of the soil around the tunnel and the consolidation is due to the unsteady state of the water flow after the tunnel excavation. The consolidation caused the deformation of the soil around the tunnel and the pressure on the lining changed. Thus the internal forces in the lining change.



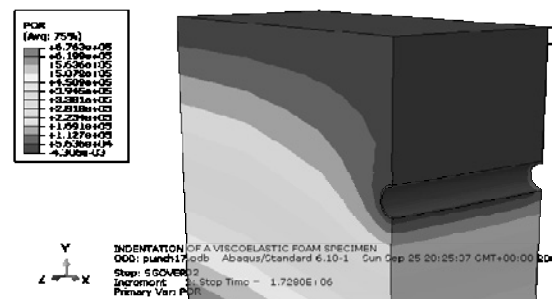
(a) Excavation length=D.



(b) Excavation length=4D.



(c) Excavation length=10D.



(d) After excavation.

Fig. 9. The pore water pressure distribution at different excavation step with permeable advance face and permeable lining.

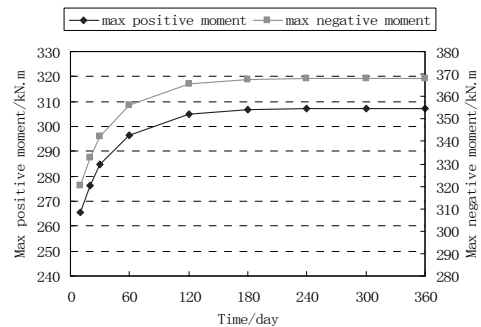


Fig. 10. The development of max moment in the lining with permeable advance face and permeable lining.

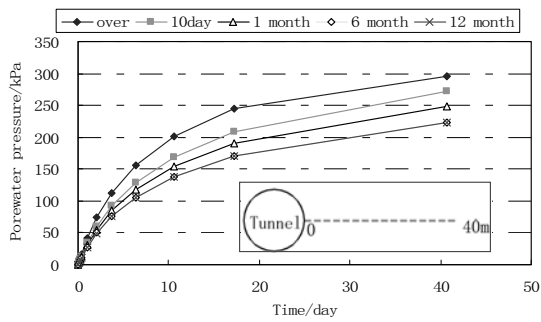


Fig. 11. The pore water pressure along the line on the right of the tunnel at different time.

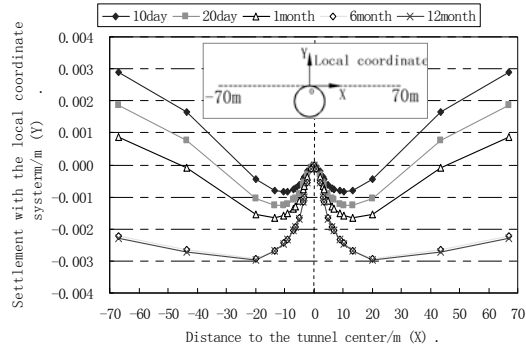


Fig. 12. The differential settlement of soil up the tunnel with the local coordinate at the roof of tunnel.

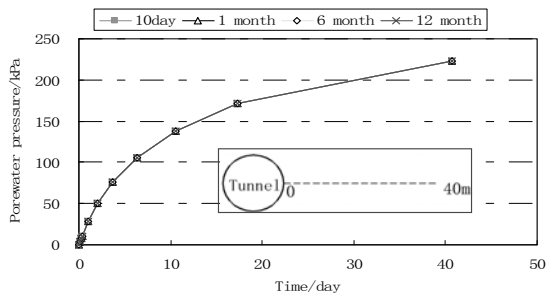


Fig. 13. The pore water pressure along the line on the right of the tunnel at different time ( $K=1 \times 10^{-6}$ ).

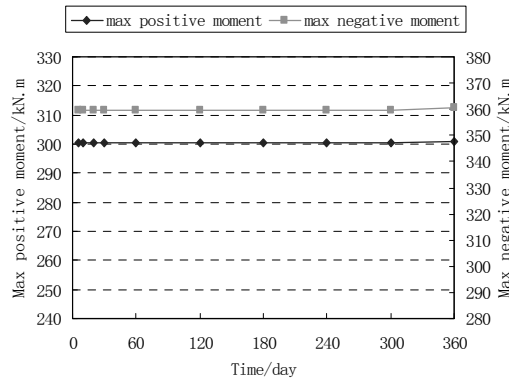
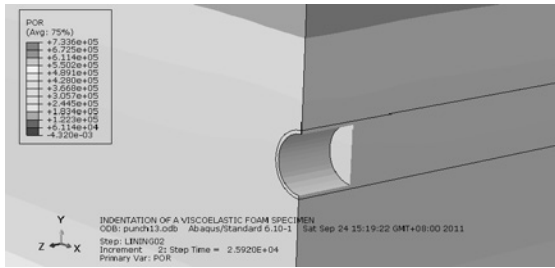
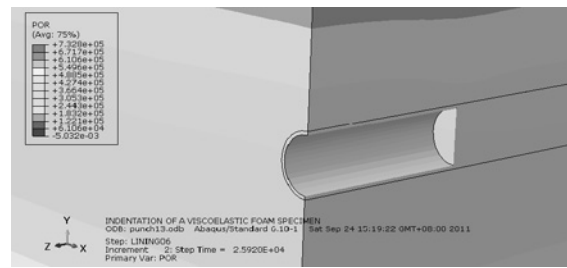


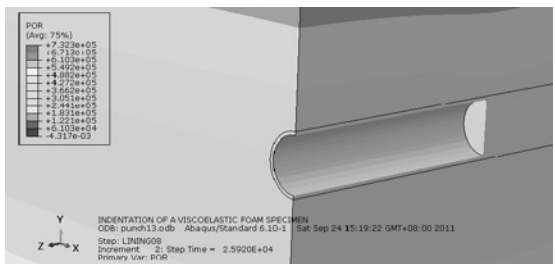
Fig. 14. Internal forces in the lining with permeable advance face and permeable lining ( $K = 1 \times 10^{-6}$ ).



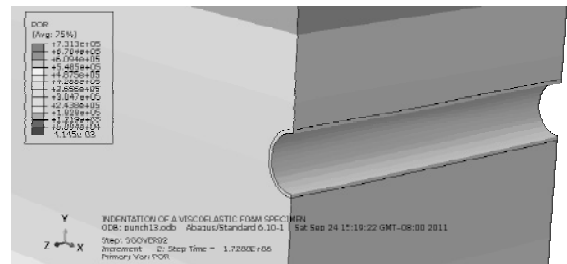
(a) Excavation length=2D.



(b) Excavation length=6D



(c) Excavation length=8D



(d) After the tunnel excavation

Fig. 15. The pore water pressure distribution at different time with impermeable advance face and impermeable lining.

The changes of the internal forces in the lining after tunnel excavation are influenced by the boundary condition of the advance face and the lining. When the lining is impermeable the internal forces in the lining

changes a little (no larger than 7 kN·m) after tunnel excavation. When the advance face is permeable the internal forces increased and when the advance face is impermeable the internal forces decreased. This is due to

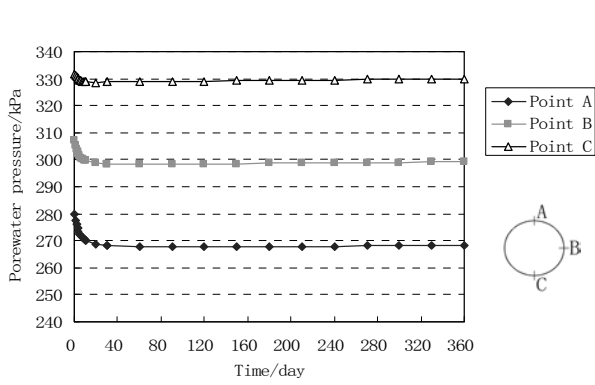


Fig. 16. Pore-water pressure around the lining.

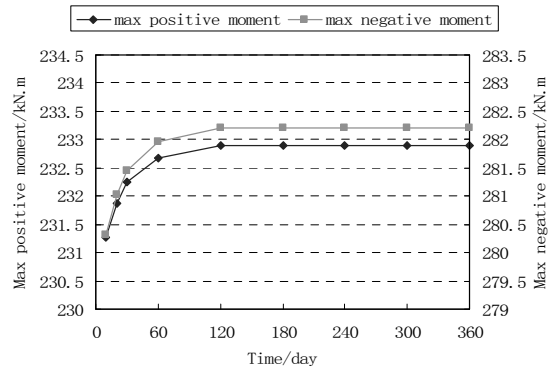


Fig. 17. Internal forces in the lining at different time.

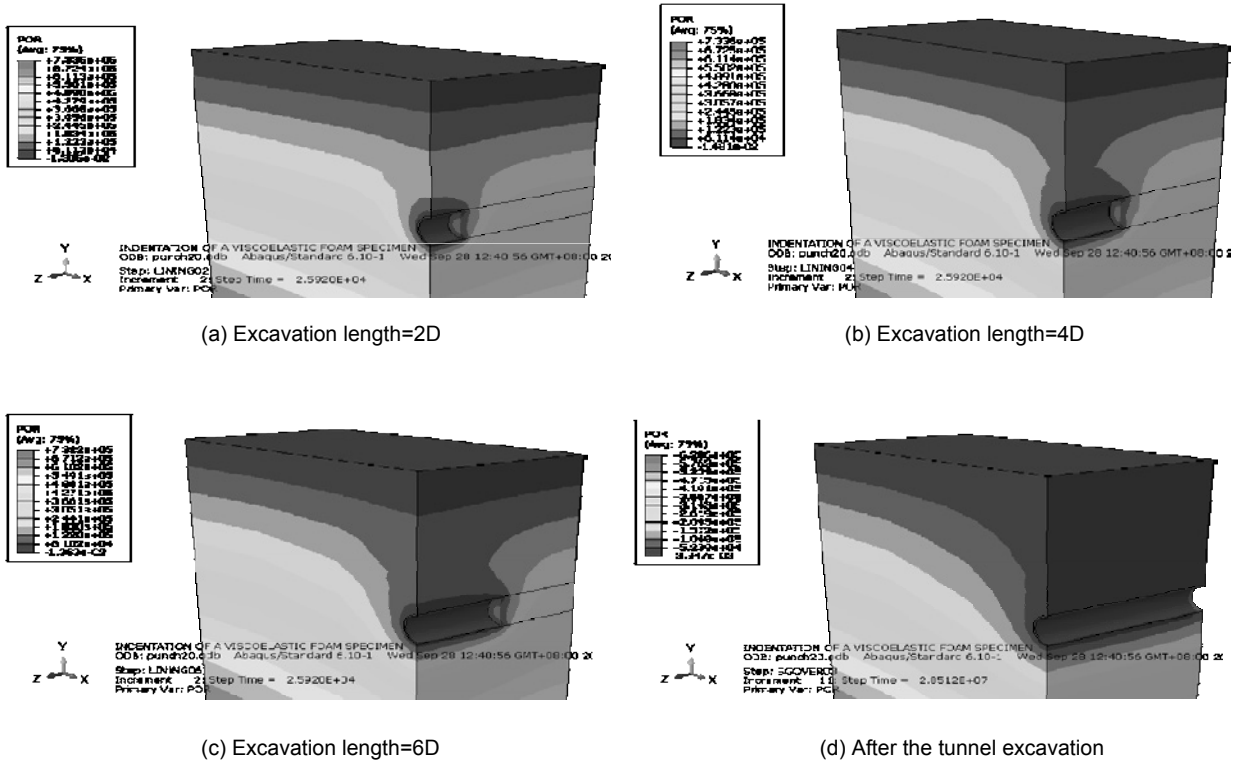


Fig. 18. The pore water pressure distribution at different time with impermeable advance face and permeable lining.

the positive or negative pore water pressure caused by the tunnel excavation around the tunnel.

When the lining is permeable the increase value is dramatic (larger than 70 kN·m). This is due to the decrease of the pore water pressure around lining. The permeable lining can produce a steady state water flow around the lining but it needs some time after the lining is installed. The decrease of pore water pressure induced the deformation of soil and the increase of internal forces in the lining. When the advance face is permeable the pore water pressure around the tunnel can be reduced by the advance face. When the advance face is impermeable the pore water pressure is reduced by the permeable lining only. So when the advance face is

impermeable, the increased internal forces in the lining after tunnel excavation are larger than the result when the advance face is permeable.

It should be pointed out that when the soil permeability is large, pore pressure dissipation occurs practically simultaneously with tunnel excavation, and the water flow around the tunnel reaches steady state immediately. Thus no time-dependency can be observed after tunnel excavation. So that when the tunnel is buried in large permeably soil the internal forces in the lining will be constant after tunnel excavation without increasing with time.



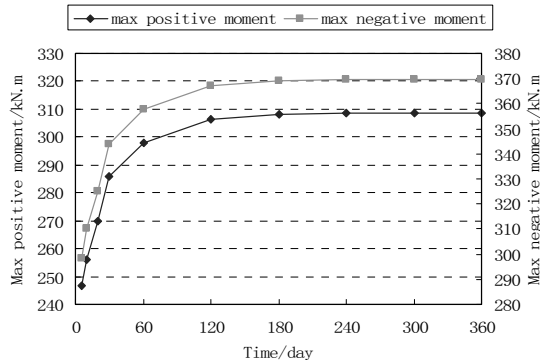


Fig. 19. The development of max moment in the lining with impermeable advance face and permeable lining

#### 4. Conclusions

The effect of boundary conditions of advance face and lining is investigated by 3D coupled mechanical and hydraulic numerical simulation. The following conclusions can be drawn from the calculation results:

1. The changes of the internal forces in the lining are due to the consolidation of the soil around the tunnel and the consolidation is due to the unsteady state of the water flow after the tunnel excavation. The consolidation caused the deformation of the soil around the tunnel and the pressure on the lining changed and the internal forces in the lining increased or decreased.
2. When the lining is impermeable the internal forces in the lining changes a little (no larger than 7 kN•m) after tunnel excavation. When the advance face is permeable the internal forces increased and when the advance face is impermeable the internal forces decreased. This is due to the positive or negative pore water pressure caused by the tunnel excavation around the tunnel.
3. When the lining is permeable the increase value is dramatic (larger than 70 kN•m). This is due to the decrease of the pore water pressure around lining to formulate a steady state water flow around the tunnel. And when the advance face is impermeable, the increased internal forces in the lining after tunnel excavation are larger than the result when the advance face is permeable.
4. When the tunnel is buried in large permeably soil the internal forces in the lining will be constant after tunnel excavation without increasing with time. Because the pore pressure dissipation occurs practically simultaneously with tunnel excavation and the water flow around the tunnel reaches steady state immediately.

#### Acknowledgements

This paper was supported by the faculty research fund of Six major talent peak in Jiangsu province. This support is gratefully acknowledged.

#### References

- ABAQUS Consulting Group, 2008. ABAQUS User's Guide: 192.
- Anagnostou, G. and Kovári, K., 1996. Face stability conditions with earth pressure balanced shields. *Tunnelling and Underground Space Technology*, **11** (2): 165-173.
- Anagnostou, G., 2005. The influence of tunnel excavation on the hydraulic head. *International J. Analytical Methods in Geomechanics*, **19** (10): 725-746.
- Atkinson, J.H. and Mair, R.J., 1983. Loads on leaking and watertight tunnel linings, sewers and buried pipes due to groundwater. *Geotechnique*, **33** (3): 341-344.
- Galli, G., Grimaldi, A. and Leonardi, A., 2004 Three-dimensional modelling of tunnel excavation and lining. *Computers and Geotechnics*, **31**: 171-183.
- Thomas, K. and Gunther, M., 2006. On the influence of face pressure, grouting pressure and TBM design in soft ground tunnelling. *Tunnelling and Underground Space Technology*, **21**: 160-171.
- Lee, I.M. and Nam, S.W., 2004. Effect of tunnel advance rate on seepage forces acting on the underwater tunnel face. *Tunnelling and Underground Space Technology*, **19** (11): 273-281.
- Lee, I.M. and Nam, S.W. 2001. The study of seepage forces acting on the tunnel lining and tunnel face in shallow tunnels. *Tunnelling and Underground Space Technology*, **16** (1): 31-40.
- Lee, K.M. and Rowe, R.K., 1990. Finite element modelling of the three-dimensional ground deformations due to tunnelling in soft cohesive soils: Part I – Method of analysis. *Computers and Geotechnics*, **10** (2): 87-109.
- Mansour, M., 1996. Three-dimensional numerical modelling of hydroshield tunnelling. Ph.D. Thesis, University of Innsbruck (unpublished).
- Mroueh, H. and Shahrour, I. 2008. A simplified 3D model for tunnel construction using tunnel boring machines. *Tunnelling and Underground Space Technology*, **23** (6): 38-45.
- O' Reilly, M.P., Mair, R.J. and Alderman, G.H., 1991. Long-term settlements over Tunnels. An eleven-year study at Grimsby. *Tunnelling'91, Inst. of Mining and Metallurgy, London*: 55-64.

- Park, K.H., Owatsiriwong, A. and Lee, J.G., 2008. Analytical solution for steady-state groundwater inflow into a drained circular tunnel in a semi-infinite aquifer: a revisit. *Tunnelling and Underground Space Technology*, **23** (6): 206-209.
- Ponlawich, A., Jae-Hyeung, J. and Chang-Yong, K., 2009. Effect of drainage conditions on pore-water pressure distributions and lining stresses in drained tunnels. *Tunnelling and Underground Space Technology*, **24** (5): 376-389.
- Ramoni, M. and Anagnostou, G., 2011. The interaction between shield, ground and tunnel support in TBM tunnelling through squeezing ground. *Rock Mechanics and Rock Engineering*, **44**: 37-61.
- Schweiger, H.F., Pottler, P.K. and Steiner, H., 1991. Effect of seepage forces on the shotcrete lining of a large undersea cavern. *Computer Methods and Advances in Geomechanics*, Balkema, Rotterdam: 1503-1508.
- Shin, J.H., Potts, D.M. and Zdravkovic, L., 2005. The effect of pore-water pressure on NATM tunnel linings in decomposed granite soil. *Can. Geotech. Journal*, **42**: 1585-1599.
- Swoboda, G., Abu-Krishna, A., 1999. Three-dimensional numerical modelling for TBM tunnelling in consolidated clay. *Tunnelling and Underground Space Technology*, **14** (3): 327-333.